Microstructural characteristics of planar granular solids

Takashi Matsushima* and Raphael Blumenfeld†

*Department of Engineering Mechanics and Energy, University of Tsukuba, Tsukuba, Ibaraki, 305-8573, Japan
†Earth Science and Engineering, Imperial College London, London SW7 2AZ, UK
Cavendish Laboratory, Cambridge University, JJ Thomson Avenue, Cambridge CB3 0HE, UK

Abstract. The microstructure of granular materials is the main factor determining their macroscopic behaviour. We study systematically the statistical characteristics of volume elements (called quadrons) of microstructures of mono- and polydisperse planar disc packs granular and report a number of new results. The packs analysed were of different intergranular friction coefficients ,μ, contained about 20,000 discs each and were brought to mechanical equilibrium under identical isotropic compression stresses from three different initial states: loose, intermediate and dense. Our findings are the following. (i) The rattlers volume fraction ϕ_r is not affected by the disc size distribution (DSD). (ii) Excluding the rattlers, we find that the relation between the packing fraction ϕ' and the mean coordination number $\bar{z}$ is independent of the initial state. Together with result (i), this allows us to separate the effects of the DSD and the initial state on the microstructure. (iii) We relate analytically $\bar{z}$, ϕ' and the (normalised) mean quadron volume $\bar{v}'$. (iv) Combining (iii) and a relation between $\bar{z}$ and the mean cell order, $\bar{e}$, derived from Euler's topological relation, we show that (ii) is a result of the geometrical relation between $\bar{v}'$ and $\bar{e}$. (v) The probability density function of the quadron volumes, normalised by $\bar{v}'$, is universal for all the studied systems and it can be fit reasonably well by a Γ distribution.

Keywords: granular solid, microstructure, quadron, packing fraction
PACS: 45.70.Cc,structure, 61.43.-j,78.40.Pg,81.05.Rm

INTRODUCTION

In spite of the key role that granular materials play in human society and the sensitivity of significance of their their mechanical properties to the microstructures, the structure-mechanics relation is yet to be understood [1, 2, 3, 4, 5]. Understanding the pore-scale statistics in granular solid is also important to their transport properties [6, 7] and to a range of applications, e.g. in planetary science, materials, geotechnical and energy engineering.

Here we use the quadron description [8, 9] to study the microstructural characteristics of numerically-generated planar granular solids, through the statistics of the quadron volumes. Several packs were prepared by the same procedure, varying interparticle friction, initial generation states and disc size distribution and we studied the effects on microstructural properties: quadron volume distribution, mean coordination number, and packing fraction.

QUADRON: A BASIC VOLUME ELEMENT

The quadron description, proposed in [8, 9, 10] involves elementary volume elements, quadrons, that tessellate the granular space and are used to quantify the local structure [11, 12]. This description has been used to construct a stress theory of isostatic granular materials [8] and a statistical mechanical formalism [9, 10, 13]. In contrast to other definitions of volume elements, e.g. Volonoi-based tesserations [4], quadrons preserve the connectivity information, since their construction is based on the force-carrying intergranular contacts. They also make possible an unambiguous local quantitative description of the microstructure.

Fig. 1 illustrates the 2D quadron construction. First, one defines the centroids of grains g and cells c as the mean position vectors of the contact points around them, respectively. Then, the contact points around every grain are connected to make polygons, whose edges are vectors, $\vec{r}^{gc}$, that circulate the grains clockwise. Next, vectors $\vec{R}^{gc}$ are extended from the grain centroids to the centroids of the cells c surrounding them. A quadron is, generically, the quadrilateral whose diagonals are the vectors $\vec{r}^{gc}$ and $\vec{R}^{gc}$. Since every pair gc corresponds to exactly one quadron, we denote a quadron by q for convenience. The quadron's volume is computed as $V^q = | \vec{r}^q \times \vec{R}^q | /2 = (r^q_x R^q_y - r^q_y R^q_x)/2$

NUMERICAL EXPERIMENTS

For our numerical experiments we used the Discrete Element Method (DEM) ([14, 15]). It consists of using an incremental time marching scheme, wherein the motion of each disc is computed by Newton's second law. We postulate a repelling harmonic interaction between discs with a normal and tangential spring constants, k_n and

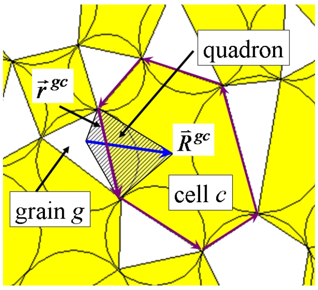

FIGURE 1. Quadrons (shaded) and cells (yellow).

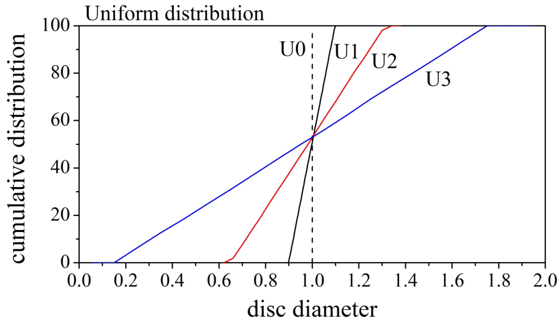

FIGURE 2. Uniform DSDs for four systems: U0, U1, U2 and U3. U0 has a monodisperse DSD.

k_s, activated upon contact and overlap between discs. We set $k_s/k_n = 1/4$. We prepared four sets of systems, each with a different cumulative disc size distributions (DSDs), U0, U1, U2, and U3, shown in Fig. 2. U0 has a mono-dispersed DSD while U1 to U3 are uniform with different ranges.

The packing protocol of our systems is as follows. First, we construct two random almost jammed packs of about 20,000 discs, for each material in a double periodic domain. One system is a loose pack, of packing fraction $\phi = 0.74$, and the other is the densest unjammed pack whose packing fraction is different for different systems. The two almost jammed configurations, loose initial state (LIS) and dense initial state (DIS), are then used as initial states for the packing procedure, giving us 8 initial specimens.

Once an initial state is set, we assign all the particles a friction coefficient, μ, and apply to the system a slow isotropic stress σ_c by changing the periodic length in both directions. The stress level is limited such that the average overlap of discs is $\delta = \sigma_c/k_n = 10^{-5}$. No gravitational force is applied and the compression continues until the fluctuations of both grain positions (per mean grain diameter) and inter-granular forces (per mean average contact force) are below very small thresholds - 10^{-9} and 10^{-6}, respectively. This procedure is carried out for each initial state at five different values of the inter-granular friction coefficients: $\mu = 0.01, 0.1, 0.2, 0.5$ and 10, giving altogether 40 different assemblies. Hereafter we denote them as, e.g. U0-LIS-0.01.

STRUCTURAL ANALYSES

For all the systems we computed the packing fractions ϕ, mean coordination numbers $\bar{z}$ and the statistical properties of quadrons. As expected, $\bar{z}$ is mainly controlled by μ, as shown in Fig.3. The initial state has hardly any effect and nor does the DSD, except in the monodisperse systems (U0), where the difference is probably due to crystallisation. To determine $\bar{z}$, we ignore 'rattlers', which are discs with one or no force-carrying contact, because they do not contribute to the structural stability. The values of $\bar{z}$ ranges between 3 and 4 in U1-U3 systems, consistent with the isostatic theory for random packs [16, 17].

We show the relations between $\bar{z}$ and ϕ for all the systems in Fig. 4. The packing fractions of the U3 systems are larger than in U1 and U2, which is due to the different DSDs - with higher fractions of small discs one can fill pores more effectively [18]. The U0 systems exhibit a different trend because of their crystalline regions.

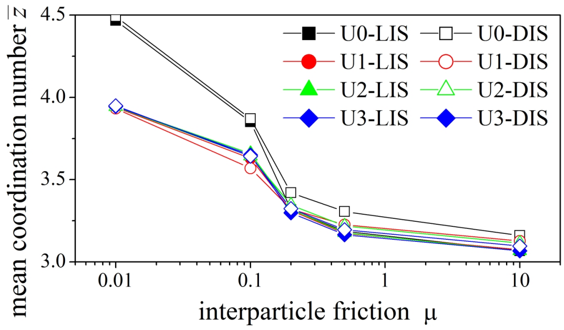

FIGURE 3. The collapse of $\bar{z}(\mu)$ for all systems except U0.

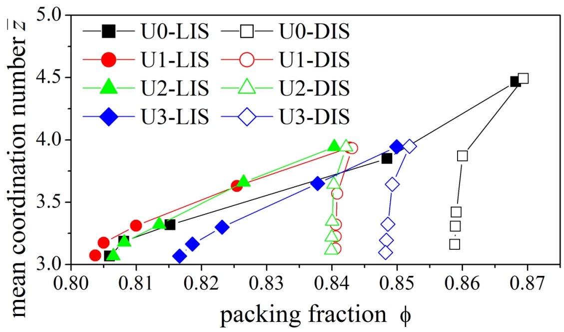

FIGURE 4. The raw relations $\bar{z}(\phi)$ (rattlers included).

Fig. 5 shows some examples of the granular packs in static equilibrium together with their cell structures. In general, the larger the interparticle friction the larger the cells, as expected. Rattlers, which do not contribute to the mechanical stability, exist in all systems and affect the packing fraction. The packing fractions in Figs. 5(a) and 5(b) are very similar, but the cells in 5(b) are typically larger, giving different $\bar{z}$s. We note that Figs. 5(b) and (c), whose $\bar{z}$s are similar, seems to have similar cell sizes although their DSDs and packing fractions are quite different. Fig. 5(d) clearly shows that the smooth monodisperse packs develop crystalline regions. The cell size is closely related to the cell order, defined as the number of edges around the cell polygon, and to its quadron volumes, as we discuss later.

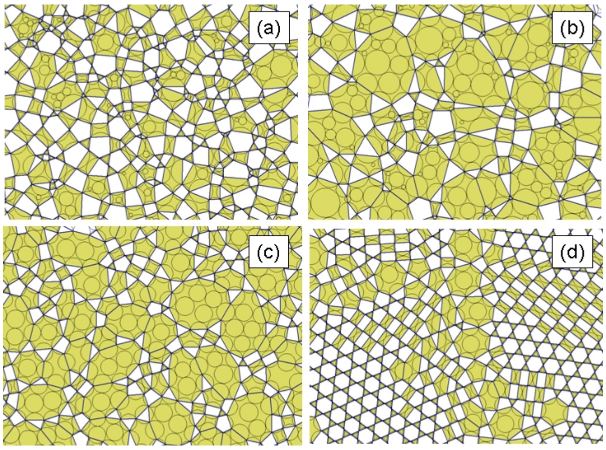

FIGURE 5. Examples of the cell structures: (a) U3-LIS0.01 ($\bar{z}$=3.94, $\phi = 0.845$); (b) U3-DIS10 ($\bar{z}$=3.10, $\phi = 0.848$); (c) U1-LIS10 ($\bar{z}$=3.07, $\phi = 0.804$); (d) U0-LIS0.01 ($\bar{z}$=4.47, $\phi = 0.868$).

Since we ignore rattlers both in the calculation of $\bar{z}$ and in the quadron construction, it is natural to consider the rattler-free packing fraction, ϕ'. It is defined as $\phi' = N_g' \bar{V}_g'/V$, where N_g' and $\bar{V}_g'$ are the number of discs and the mean disc volume after removing rattlers, and V is the total system volume. Fig. 6 shows the relation between $\bar{z}$ and ϕ'. Except for monodisperse systems, the effect of the initial state has disappeared almost completely, indicating that the difference in the packing fraction, often attributed to the initial state, can be traced to the difference in the rattlers fraction. To explore this issue, we identify the rattlers volume fraction, $\phi_r = 1 - N_g'\bar{V}_g'/N_g\bar{V}_g$, which gives a relation between ϕ' and ϕ,

$$\phi = \frac{\phi'}{1-\phi_r} \tag{1}$$

Plotting $\bar{z}$ against ϕ_r for all systems (Fig. 7), we note that, for $\mu = 0.01$, all systems have an almost identical value of ϕ_r, except for the monodisperse system. Taken together with Eq. 1, this means that the DSD affects only ϕ', not ϕ_r. It follows that the initial state, which does not appear in Fig. 6, affects only ϕ_r. In turn, this shows that we can separate the effects of the DSD and the initial state on the packing fraction - the former affects ϕ' and the latter affects ϕ_r.

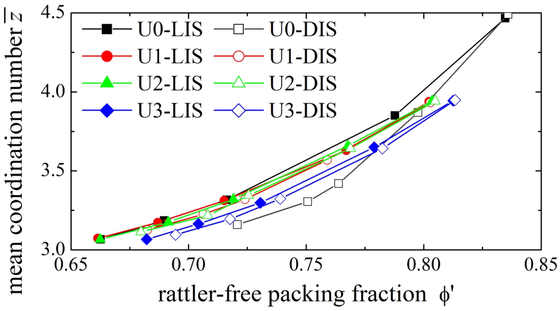

FIGURE 6. $\bar{z}$ vs. ϕ' depends only on the DSD.

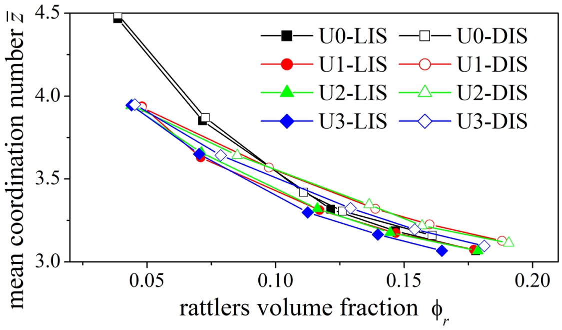

FIGURE 7. Relation between the mean coordination number $\bar{z}$ and the rattlers volume fraction ϕ'

We next derive the following useful relation for rattler-free packs,

$$\phi' = \frac{N_g'\bar{V}_g'}{V} = \frac{N_g'\bar{V}_g'}{N_q\bar{V}_q} = \frac{1}{\bar{v}'\bar{z}} \tag{2}$$

where $\bar{v}' = \bar{V}_q/\bar{V}_g'$ is the mean quadron volume, normalised by the mean grain volume, and N_q is the total number of quadrons. This relates $\bar{v}'$ directly to $\bar{z}$ and ϕ'. Combining this relation with an identity between $\bar{z}$ and the mean cell order $\bar{e}$, based on the Euler's topological relation [19],

$$\bar{e} = \frac{2\bar{z}}{\bar{z}-2} + O\left(\frac{1}{\sqrt{N}}\right) \tag{3}$$

where the rightmost term is a (negligible) boundary correction, we see that $\bar{v}'$ is a direct function of $\bar{e}$ and ϕ'.

In Fig. 8 we plot $\bar{v}'$ against $\bar{e}$ for all the systems. All the curves collapse nicely including all U0s. The small deviations are due to the effect of the DSD on the

$\phi' - \bar{z}$ relation (Fig. 6). The relation between $\bar{v}'$ and $\bar{e}$ is key to the understanding of the structural characteristics; we can see from Fig. 1 that the quadron volume v_q is related to the cell order via the increase of R^{gc} with cell order. To illustrate this effect, we approximate the cells as regular polygons. Then the quadron volume is $v^{RPC} = \cot(\pi/e)/\pi$. As observed from Fig. 8, this relation gives a tight upper bound to the numerical results. Although this approximation ignores the effects of cell shapes, DSD, frequency of cell orders and so on, the dependence of $\bar{v}'$ on $\bar{e}$ is arguably the origin of the relation $\bar{z}(\phi')$ in Fig. 6.

The PDFs of the normalised quadron volumes, $u = v'/\bar{v}' = V_q/\overline{V_q}$, collapse nicely to one master curve for all systems with the same DSD, as seen in Fig. 9 for 10 U3 systems. This master curve is fitted well by the Γ distribution, $P(u) = \alpha^{\alpha} u^{\alpha-1} e^{-\alpha u}/\Gamma(\alpha)$, with $\alpha = 2$. Repeating the same for U0-U2 systems, we find the same result with α increasing slightly with decreasing polydispersity. Nevertheless, the collapse is not as sharp because the fluctuations of v' cannot be neglected [11].

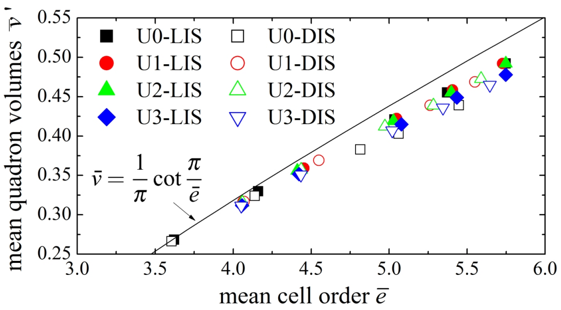

FIGURE 8. $v'(\bar{e})$ collapse to one curve for all systems.

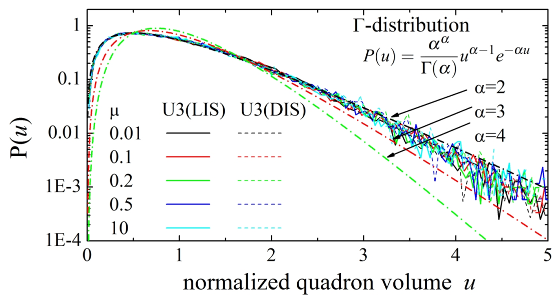

FIGURE 9. PDF of the normalized quadron volume $u = V_q/\overline{V_q}$ for 10 U3 systems

CONCLUSIONS

We studied the structural properties of the disc assemblies, varying the interparticle friction, disc size distribution and initial state. We found that the rattlers are essential to understanding the packing fraction and structural characteristics. The mean quadron volume is primarily controlled by the mean cell order, which also determines the rattler-free packing fraction with respect to the mean coordination number. Relating these variables, as we have done, allowed us to normalise the quadron volume distributions [19] and collapse them to a master curve. This collapse shows that the structures of granular systems are determined by the DSD, while the initial state and friction coefficient can be scaled away.

ACKNOWLEDGMENTS

TM is grateful for the financial support from Kajima Foundation for his sabbatical in Cavendish Laboratory, University of Cambridge from Aug. 2011 to Aug. 2012.

REFERENCES

1. J. Knight, C. Fandrich, C. Lau, H. Jaeger, and S. Nagel, *Physical review E* **51**, 3957–3963 (1995).
2. L. E. Silbert, D. Ertas, G. S. Grest, T. C. Halsey, and D. Levine, *Phys. Rev. E* **65**, 031304 (2002).
3. T. Aste, T. Di Matteo, M. Saadatfar, T. J. Senden, M. Schröter, and H. L. Swinney, *EPL* **79**, 24003 (2007).
4. C. Song, P. Wang, and H. Makse, *Nature* **453**, 629–632 (2008).
5. A. Tordesillas, D. M. Walker, and L. Q., *Phys. Rev. E* **81**, 011302 (2010).
6. V. A. Luchnikov, N. N. Medvedev, L. Oger, and J.-P. Troadec, *Phys. Rev. E* **59**, 7205 (1999).
7. H.-J. Vogel, and K. Roth, *Journal of Hydrology* **272**, 95–106 (2003).
8. R. C. Ball, and R. Blumenfeld, *Phys. Rev. Lett.* **88**, 115505 (2002).
9. R. Blumenfeld, and S. Edwards, *Phys. Rev. Lett.* **90**, 114303 (2003).
10. R. Blumenfeld, and S. Edwards, *Euro. Phys. J. E* **19**, 23 (2006).
11. G. Frenkel, R. Blumenfeld, Z. Grof, and P. King, *Phys. Rev. E* **77**, 041304 (2008).
12. G. Frenkel, R. Blumenfeld, P. King, and M. Blunt, *Adv. Eng. Mat.* **11**, 169 (2009).
13. R. Blumenfeld, J. F. Jordan, and S. F. Edwards, *Phys. Rev. Lett.* **109**, 238001 (2012).
14. P. A. Cundall, and O. D. L. Strack, *Geotechnique* **29**, 47–65 (1979).
15. T. Matsushima, and C. S. Chang, *Granular matter* **13**, 269–276 (2011).
16. S. F. Edwards, and D. V. Grinev, *Phys. Rev. Lett.* **82**, 5397 (1999).
17. R. C. Ball, "The propagation of stress through static powders," in *Structures and Dynamics of Materials in the Mesoscopic Domain*, edited by M. Lal, R. A. Mashelkar, B. D. Kulkarni, and V. M. Naik, Imperial College Press, London, 1999.
18. S. Yerazunis, and J. Bartlett, *Nature* **195**, 33–35 (1962).
19. T. Matsushima, and R. Blumenfeld, *e-Print arXiv(cond-mat.soft* p. 1207.2988v1 (2012).